Application of diffraction wavefront tomography to GPR data from a glacier

A. Bauer[1], B. Schwarz[2], R. Delf[3] and D. Gajewski[1]

[1]Institute of Geophysics, University of Hamburg, Wave Inversion Technology (WIT)
[2]GFZ German Research Centre for Geosciences, Potsdam
[3]University of Edinburgh

Universität Hamburg
DER FORSCHUNG | DER LEHRE | DER BILDUNG

Why do diffractions matter?

- Diffractions are caused by small-scale subsurface heterogeneities, e.g.:
  - [Seismics:] faults, pinch-outs, caves...
  - [GPR:] buried small objects, caves, water intrusions in glaciers...
- Diffracted waves do not obey Snell's law, i.e. they are scattered into all directions

→ Superior illumination than reflections

→ High-resolution information about the subsurface

Outline

Introduction

Diffraction wavefront tomography

Synthetic diffraction-only GPR example

Field GPR data from a glacier

Conclusions

Outline

Introduction

Diffraction wavefront tomography

Synthetic diffraction-only GPR example

Field GPR data from a glacier

Conclusions

Introduction

- GPR data and seismic data exhibit similar wave propagation phenomena

→ Methods from applied seismics can be adapted to GPR data

- Established tomographic methods rely on reflections or diving waves and require multiple source-receiver offsets
- GPR acquisitions are often zero-offset measurements
- In zero-offset data only diffractions encode velocity information

→ Diffraction wavefront tomography: depth-velocity-model building for zero-offset data [Bauer et al., 2017, Bauer et al., 2018]

- Successful applications to multi-channel seismic [Bauer et al., 2017], single-channel seismic [Preine et al., 2020] and passive-seismic data [Diekmann et al., 2019]

From applied seismics to GPR

- The different scales have to be accounted for
- Typical magnitudes and units:

	Applied seismics	**GPR**
Distances	10^3 m $\rightarrow$ [km]	10^1 m $\rightarrow$ [m]
Traveltimes	10^0 s $\rightarrow$ [s]	10^{-7} s $\rightarrow$ [ns]
Velocities	10^3 m/s $\rightarrow$ [km/s]	10^8 m/s $\rightarrow$ [m/ns]
Frequencies	10^1 Hz $\rightarrow$ [Hz]	10^8 Hz $\rightarrow$ [MHz]
Wavelengths	10^1 m $\rightarrow$ [m]	10^{-1} m $\rightarrow$ [cm]

- Seismic velocities typically increase with depth, electromagnetic velocities decrease with depth

Outline

Introduction

Diffraction wavefront tomography

Synthetic diffraction-only GPR example

Field GPR data from a glacier

Conclusions

Wavefront attributes

- Diffraction separation by coherent wavefield subtraction [Schwarz, 2019] yields diffraction-only data
- Automatic extraction of wavefront attributes (α, R) from diffraction-only data via coherence analysis [Jäger et al., 2001]
- Hyperbolic second-order approximation of diffraction traveltime moveout

$$\Delta t^2(x_0, t_0) = \left(t_0 + 2\underbrace{\frac{\sin\alpha}{v_0}}_{\text{slope}}\Delta x\right)^2 + 2t_0\left(\underbrace{\frac{\cos^2\alpha}{v_0 R}}_{\text{curvature}}\Delta x^2\right)$$

with α: emergence angle of diffracted wavefront, R: wavefront radius, t_0: zero-offset two-way time, v_0: near-surface velocity

Wavefront tomography: image space

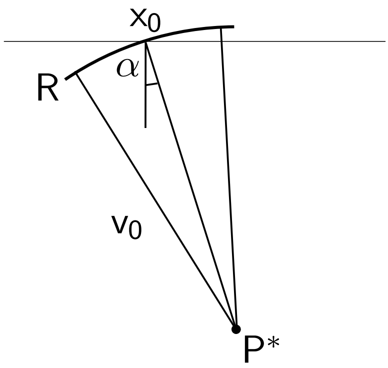

- Efficient and stable inversion scheme for smooth depth-velocity models [Duveneck, 2004, Bauer et al., 2017]
- Initial localizations P^* of data points obtained by downward kinematic ray tracing starting from (x_0, α) into constant initial model $v(x, z) = v_0$ (image space) until $t_0/2 = T_0 = 0$
- Initial localizations are quite stable because they do not depend on second-order curvature attribute R

Wavefront tomography: model space

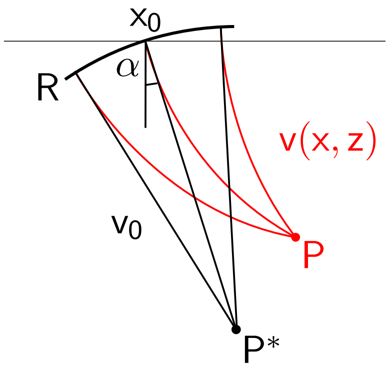

- Upward dynamic ray tracing starting from P^* yields modeled attributes (x_0, T_0, α, R)
- Goal: Find velocity model $v(x, z)$ such that $P^* = P$, i.e. the true scatterer locations

Wavefront tomography: inverse problem

- Data parameters $\mathbf{d}$: n automatically picked data points $(x_0, T_0, \alpha, R)_i$
- Velocity model is defined by B-spline functions on given grid of $n_x \times n_z$ knots
- Model parameters $\mathbf{m}$: B-spline velocity coefficients and ray start points (x, z)
- Minimize misfit between measured data $\mathbf{d}$ and modeled data $\mathbf{d}_{mod} = \mathbf{f}(\mathbf{m})$ by damped weighted least-squares

$$\Psi(\mathbf{m}) = \frac{1}{2}\left\|(\mathbf{d} - \mathbf{d}_{mod})\,\mathbf{W}\right\|_2^2 + \Lambda\left[\partial_{xx} v(x,z), \partial_{zz} v(x,z)\right]$$

- Output: smooth velocity model $v(x, z)$ and localizations of data points
- The method is equally applicable in 3D

Outline

Introduction

Diffraction wavefront tomography

Synthetic diffraction-only GPR example

Field GPR data from a glacier

Conclusions

Synthetic diffraction-only GPR example

- Synthetic diffraction-only GPR data simulating glacial setting
- 100 randomly-distributed diffractions, Gaussian noise added
- Workflow:
  1. Estimation of wavefront attributes via coherence analysis
  2. Automatic picking of data points based on their coherence
  3. Velocity inversion and scatterer localization with wavefront tomography

Synthetic example: data and attributes

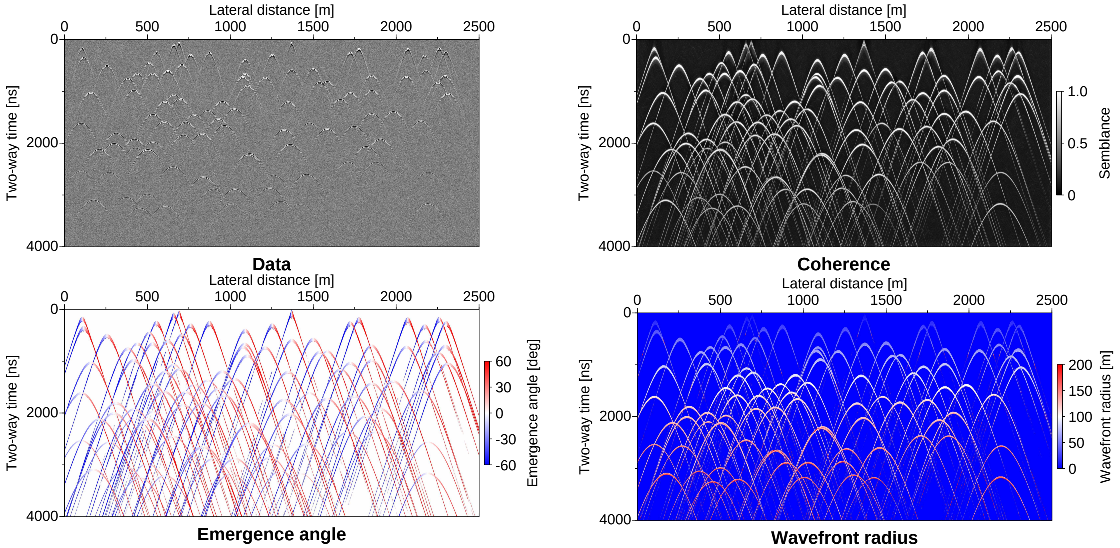

Synthetic example: picks

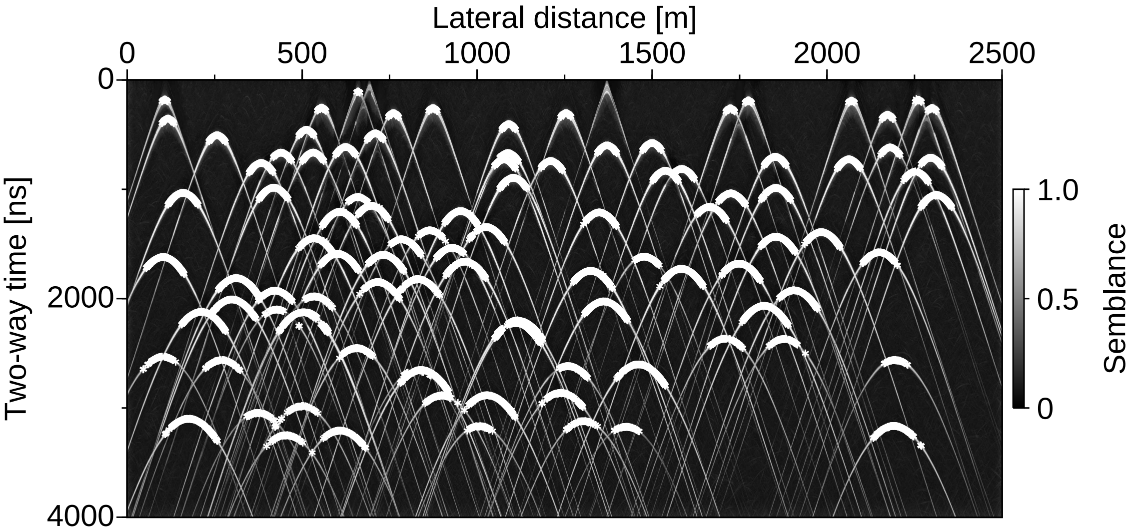

Synthetic example: initial model with localizations

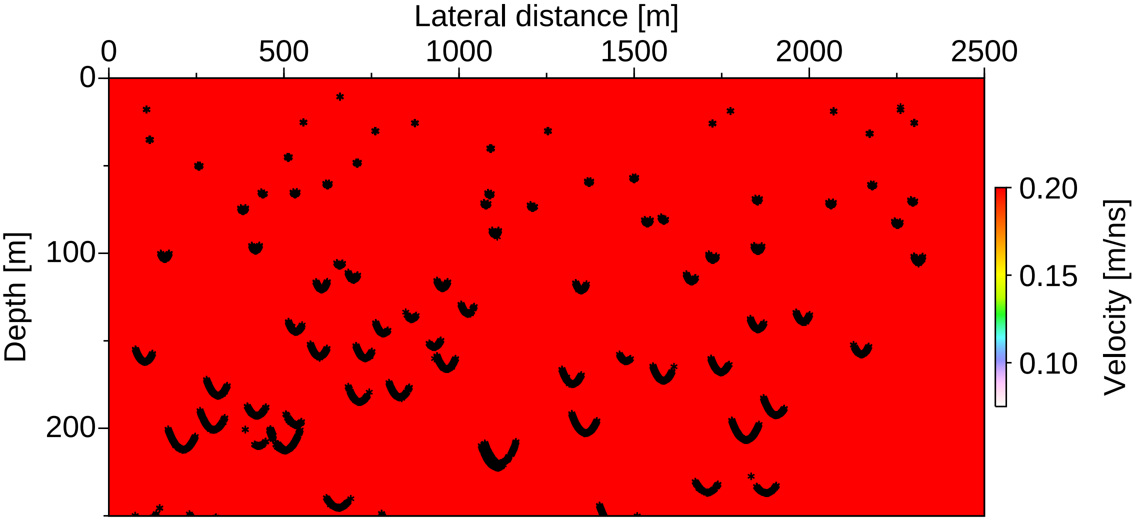

Synthetic example: final model with localizations

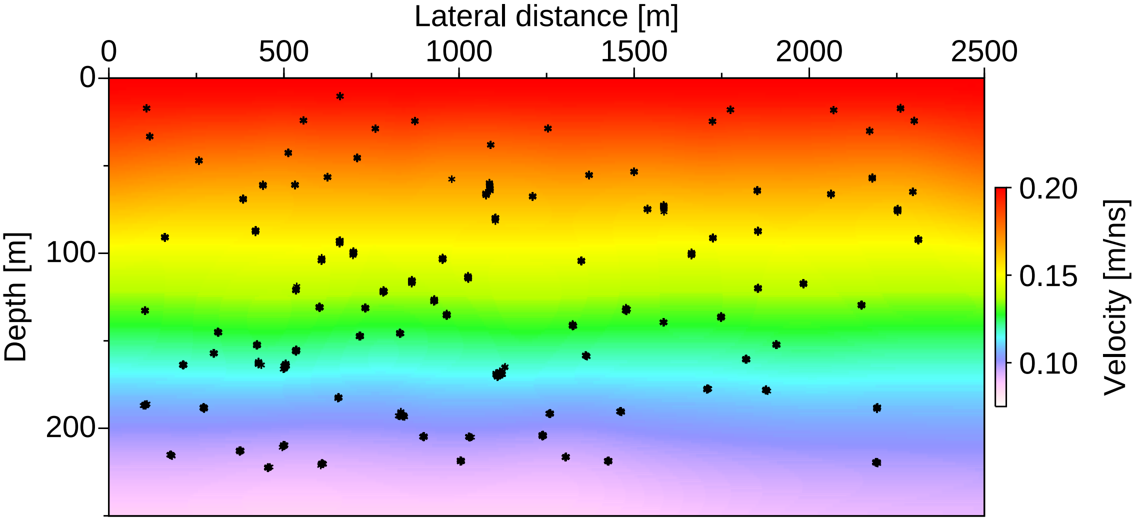

Synthetic example: correct model w/ diffractor positions

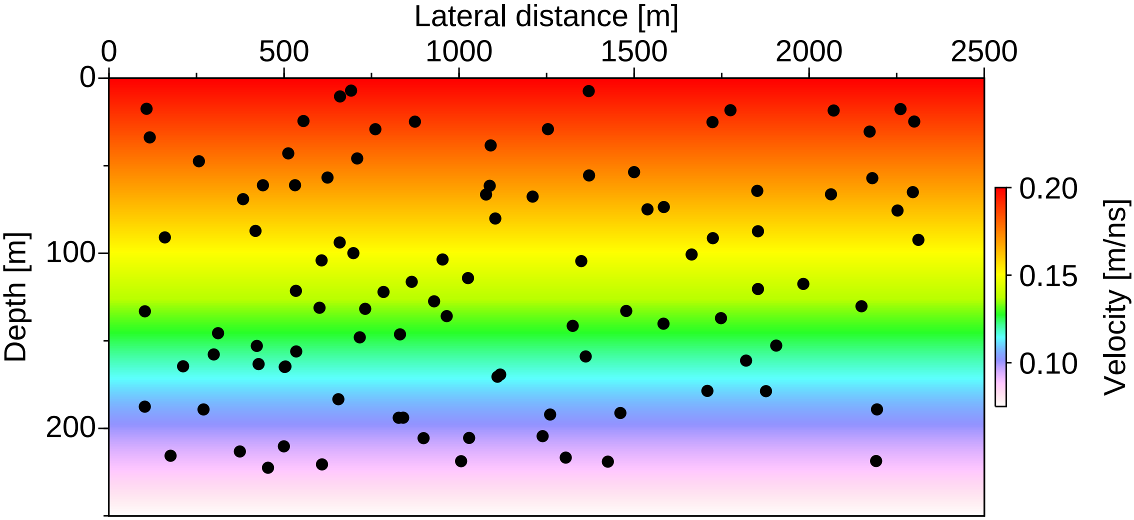

Outline

Introduction

Diffraction wavefront tomography

Synthetic diffraction-only GPR example

Field GPR data from a glacier

Conclusions

Field GPR data from a glacier

- Field GPR profile acquired at Von Post glacier, Svalbard (Norway)
- Workflow:

1. Diffraction separation via coherent wavefield subtraction
2. Estimation of wavefront attributes on diffraction-only data
3. Automatic picking of data points based on their coherence
4. Velocity inversion and scatterer localization with wavefront tomography

GPR Data from Von Post glacier, Svalbard (Norway)

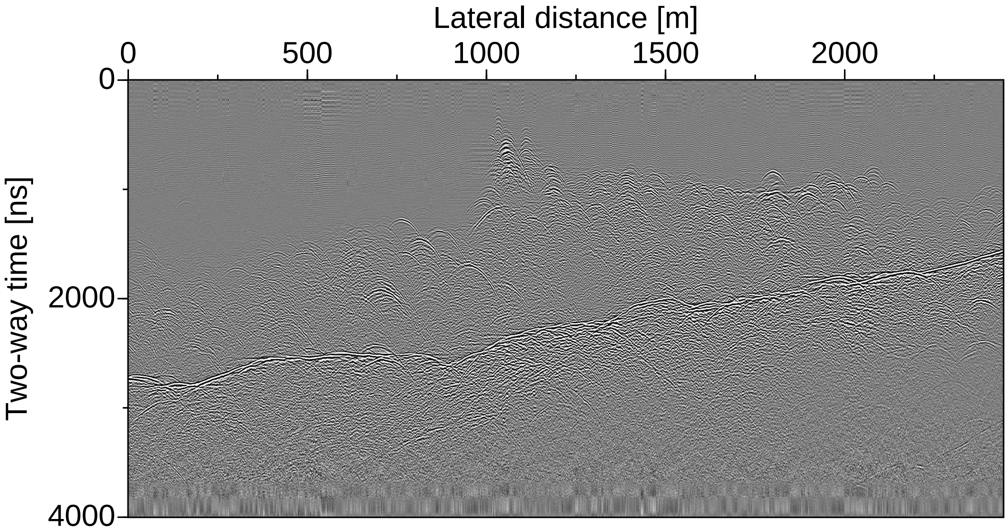

GPR Data from a glacier: diffraction coherence

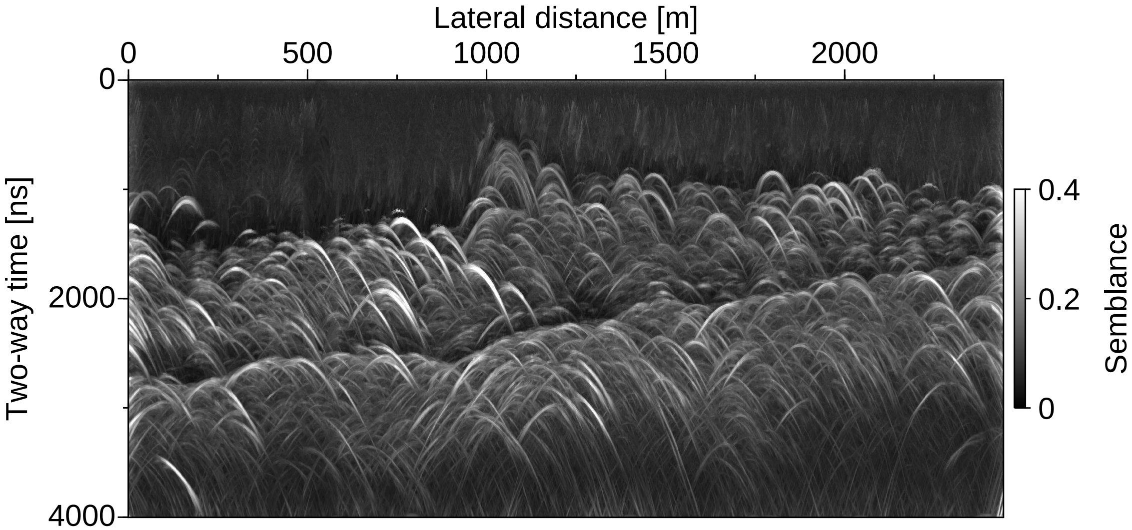

GPR Data from a glacier: emergence angle

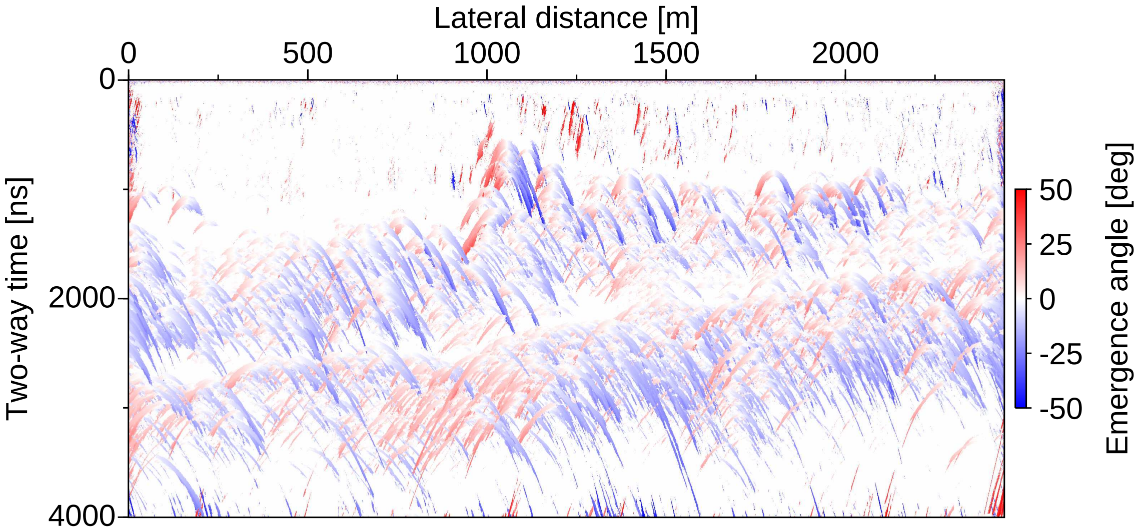

GPR Data from a glacier: wavefront radius

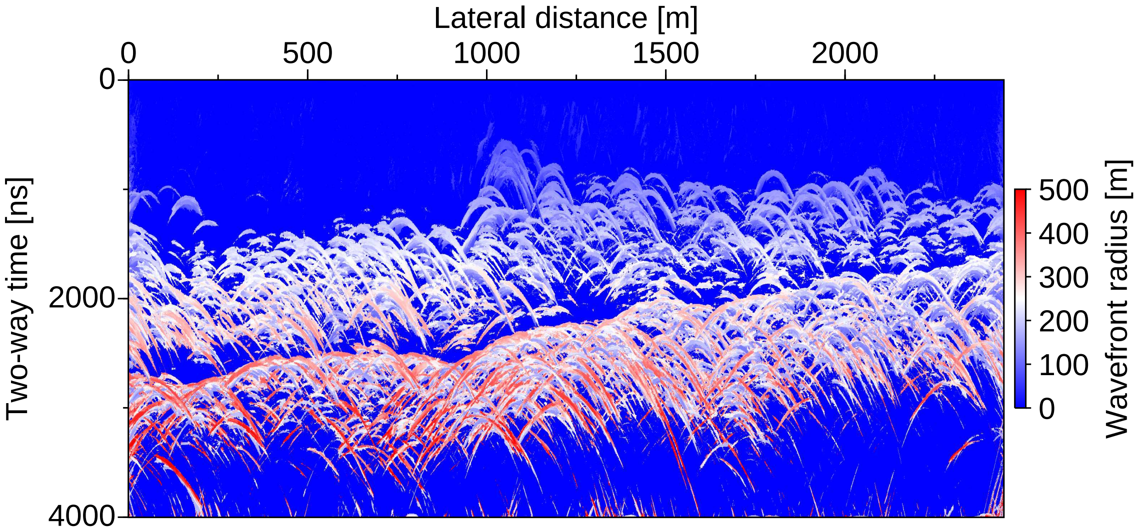

GPR Data from a glacier: picks

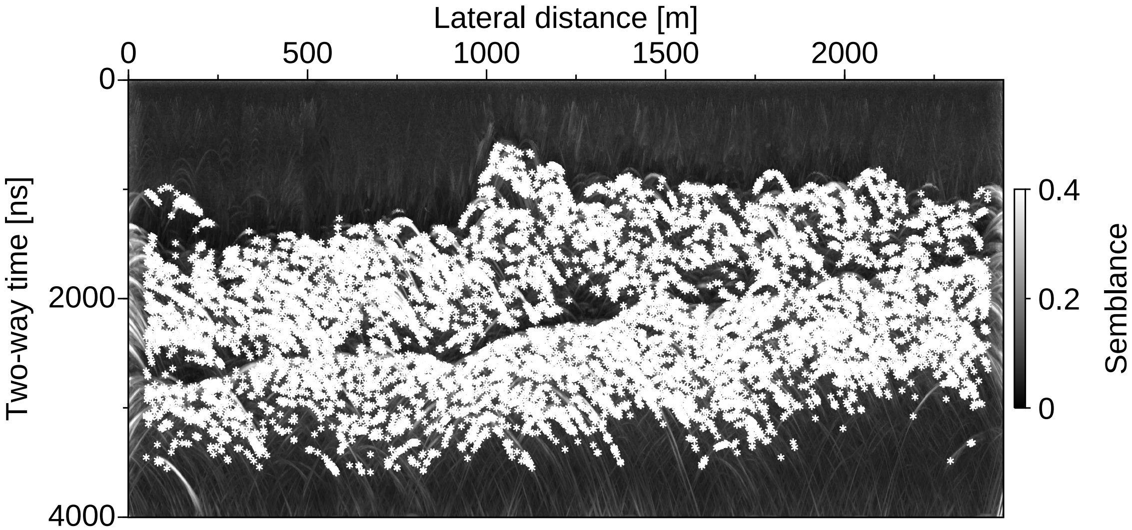

Field GPR data: initial model ($v_0 = 0.1\,\mathrm{m/ns}$)

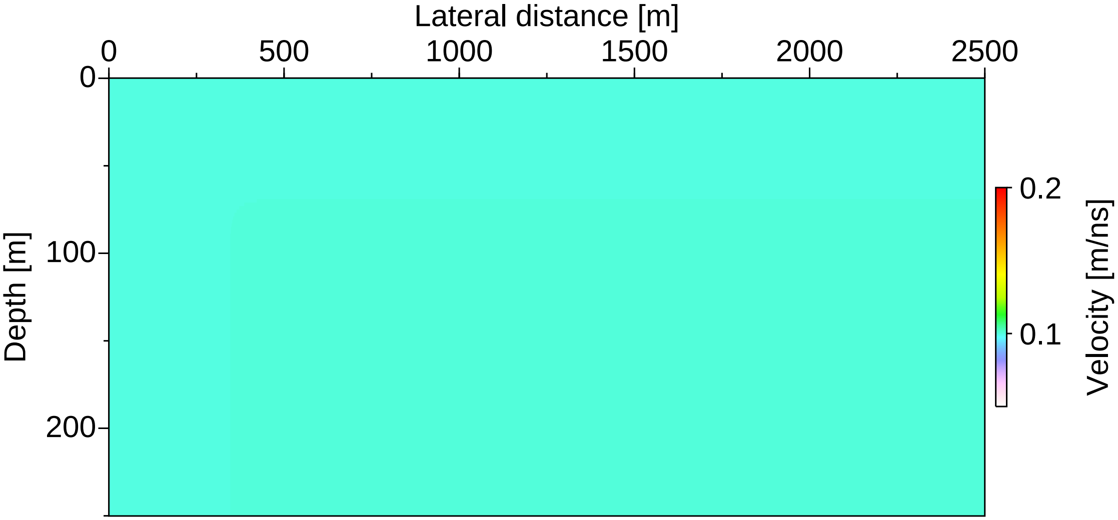

Field GPR data: initial model with localizations

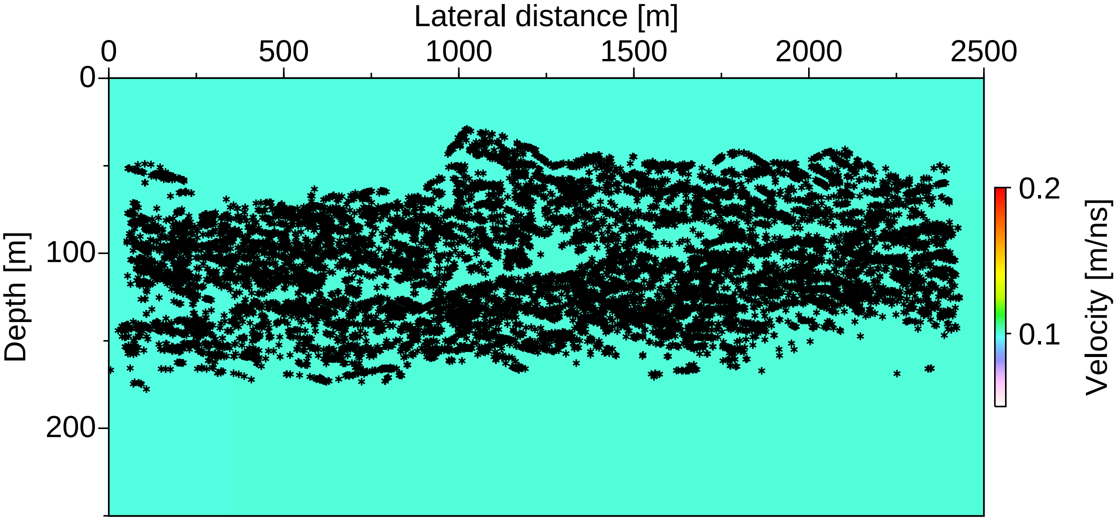

Field GPR data: initial model

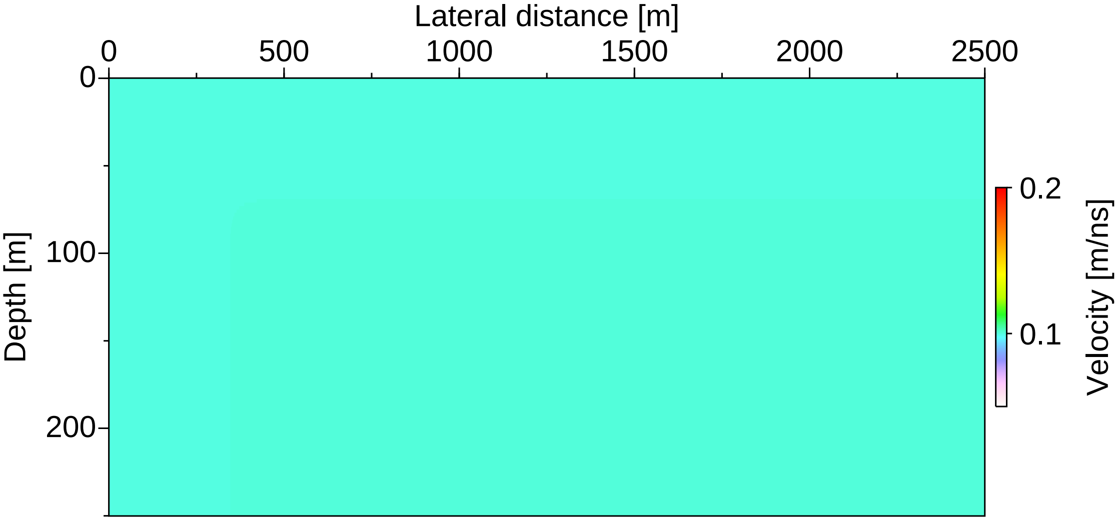

Field GPR data: final model

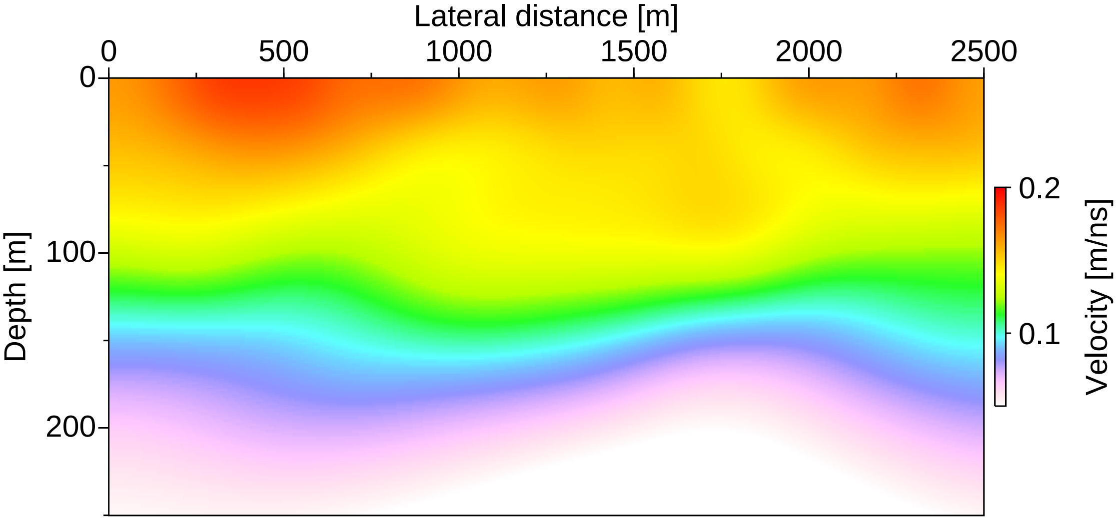

Field GPR data: final model with localizations

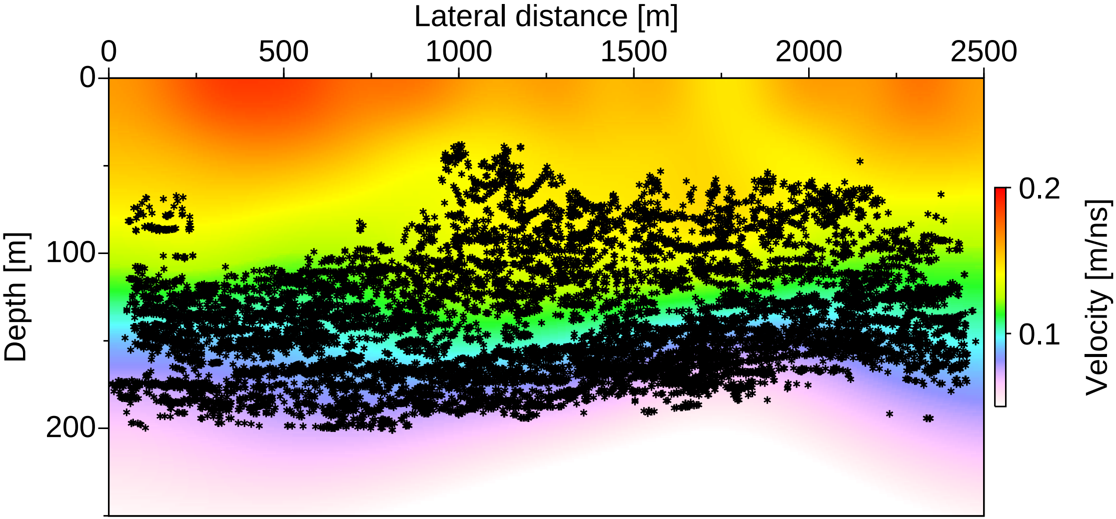

Outline

Introduction

Diffraction wavefront tomography

Synthetic diffraction-only GPR example

Field GPR data from a glacier

Conclusions

Conclusions

- Synthetic example: velocity gradient and scatterer locations correctly inverted
- Field data example: velocity model and localizations consistent with the data
- Automatized depth-velocity model building for GPR data
- Joint localization of scatterers yields additional subsurface information
- Applicable to all seismic and GPR data with rich diffracted wavefield
- No offsets required, merely sufficiently dense time sampling and trace spacing
- Estimation of second-order wavefront attributes can be challenging

Outlook

- Applications to different GPR datasets (feel free to contact me if you would like to provide data: alex.bauer@uni-hamburg.de)
- Applications to zero-offset/low-fold seismic data (P-Cable data, vintage academic data) [Bauer et al., 2020, Preine et al., 2020]
- Passive-seismic applications [Diekmann et al., 2019]
- Improved diffraction separation [Schwarz, 2019]
- Unsupervised identification and tagging of diffractions [Bauer et al., 2019b]
- Enforced focusing of diffractions during the inversion [Bauer et al., 2019a]
- Applications in 3D [Bauer et al., 2020]

Acknowledgments

- Eric Duveneck and Tilman Klüver
- Applied Seismics Group Hamburg
- Federal Ministry for Economic Affairs and Energy of Germany (BMWi, 03SX427B, 03SX504B)
- Sponsors of the WIT consortium

References I

- Bauer, A., B. Schwarz, L. Diekmann, and D. Gajewski, 2019a, Wavefront tomography with enforced diffraction focusing: Presented at the 81st EAGE Conference and Exhibition 2019.
- Bauer, A., B. Schwarz, and D. Gajewski, 2017, Utilizing diffractions in wavefront tomography: Geophysics, **82**, R65–R73.
- ———, 2018, Diffraction wavefront tomography – efficient automated velocity inversion for multi-fold and single-channel data: Presented at the 80th EAGE Conference and Exhibition 2018 - Workshops.
- ———, 2020, Velocity inversion and scatterer detection with 3D P-Cable data: submitted for SEG Technical Program Expanded Abstracts 2020.
- Bauer, A., B. Schwarz, T. Werner, and D. Gajewski, 2019b, Unsupervised event identification and tagging for diffraction focusing: Geophysical Journal International, **217**, 2165–2176.

References II

- Diekmann, L., B. Schwarz, A. Bauer, and D. Gajewski, 2019, Source localisation and joint velocity model building using wavefront attributes: Geophysical Journal International, **219**, 995–1007.
- Duveneck, E., 2004, Velocity model estimation with data-derived wavefront attributes: Geophysics, **69**, 265–274.
- Jäger, R., J. Mann, G. Höcht, and P. Hubral, 2001, Common-reflection-surface stack: Image and attributes: Geophysics, **66**, 97–109.
- Preine, J., B. Schwarz, A. Bauer, and C. Hübscher, 2020, Seismic diffraction imaging and velocity-model building in depth: A case study from the Santorini-Amorgos Tectonic Zone, South Aegean Sea: JGR: Solid Earth, under review.
- Schwarz, B., 2019, Coherent wavefield subtraction for diffraction separation: Geophysics, **84**, 1–47.